Geomechanics and Engineering, *Vol. 16, No. 4 (2018) 385-397*
DOI: https://doi.org/10.12989/gae.2018.16.4.385

Interfacial properties of composite shotcrete containing sprayed waterproofing membrane

Byungkwan Park[1], Chulho Lee[1,2], Soon-Wook Choi[2], Tae-Ho Kang[2], Jintae Kim[3], Myung-Sik Choi[3], Seokwon Jeon[4] and Soo-Ho Chang[*1,5]

[1]School of Smarty City and Construction Engineering, University of Science and Technology (UST), Goyangdae-Ro 283, Ilsanseo-Gu, Goyang-Si, Gyeonngi-Do 10223, Republic of Korea
[2]Department of Infrastructure Safety Research, Korea Institute of Civil Engineering and Building Technology, Goyangdae-Ro 283, Ilsanseo-Gu, Goyang-Si, Gyeonngi-Do 10223, Republic of Korea
[3]Silkroad T&D Co., Ltd., Woni-Ro 341, TaeanGun, Chungcheongnam-Do 32134, Republic of Korea
[4]Department of Energy Resources Engineering, Seoul National University, Gwanak-Ro 1, Gwanak-Gu, Seoul 08826, Republic of Korea
[5]Construction Startup Promotion Center, Korea Institute of Civil Engineering and Building Technology, Goyangdae-Ro 283, Ilsanseo-Gu, Goyang-Si, Gyeonngi-Do 10223, Republic of Korea

(Received February 19, 2018, Revised July 11, 2018, Accepted July 30, 2018)

Abstract. This study evaluates the interfacial properties of composite specimens consisting of shotcrete and sprayed waterproofing membrane. Two different membrane prototypes were first produced and tested for their waterproofing ability. Then composite specimens were prepared and their interfacial properties assessed in direct shear and uniaxial compression tests. The direct shear test showed the peak shear strength and shear stiffness of the composites' interface decreased as the membrane layer became thicker. The shear stiffness, a key input parameter for numerical analysis, was estimated to be 0.32-1.74 GPa/m. Shear stress transfer at the interface between the shotcrete and membrane clearly emerged when measuring peak shear strengths (1-3 MPa) under given normal stress conditions of 0.3-1.5 MPa. The failure mechanism was predominantly shear failure at the interface in most composite specimens, and shear failure in the membranes. The uniaxial compression test yielded normal stiffness values for the composite specimens of 5-24 GPa/m. The composite specimens appeared to fail by the compressive force forming transverse tension cracks, mainly around the shotcrete surface perpendicular to the membrane layer. Even though the composite specimens had strength and stiffness values sufficient for shear stress transfer at the interfaces of the two shotcrete layers and the membrane, the sprayed waterproofing membrane should be as thin as possible whilst ensuring waterproofing so as to obtain higher strength and stiffness at the interface.

Keywords: interface; spray; waterproofing; membrane; shotcrete; composite

1. Introduction

Tunnels require waterproofing to function correctly and safely. Proper waterproofing can increase the useful design life of both new and existing tunnels. If not, the leakage of water will delay the construction and degrade durability of the structure. Eventually, it will cause the unacceptable ground settlement (Nakashima *et al.* 2015).

A conventional tunnel's primary lining is typically shotcrete (sprayed concrete) with rockbolts. The secondary concrete lining is either cast in situ or sprayed. There are three main ways to waterproof a tunnel between the two layers: a sheet waterproofing membrane protected with textiles can be placed between them, the secondary lining made of watertight concrete can be sufficiently waterproof without needing any additional layer, or a sprayed waterproofing membrane can be applied directly to the primary lining (Vogel *et al*. 2017).

Sprayed waterproofing membranes can significantly improve the quality of tunnel waterproofing, especially at edges or in areas with discontinuities.

A sheet waterproofing membrane is considered to have a frictionless surface, so a lining with a sheet membrane is usually assumed to behave as a non-composite structure (Nakashima *et al.* 2015, Thomas 2009). Therefore, two linings separated by such a frictionless sheet will have to resist flexure independently, because the sheet cannot provide the necessary in-plane shear transfer between them to provide a composite action.

In contrast, a sprayed waterproofing membrane between two shotcrete layers has high adhesion and fully bonds to both, forming a composite structure with the possibility of considerably increased load sharing between them (Johnson *et al.* 2016, Nakashima *et al.* 2015, Vogel *et al.* 2017). In addition, a sprayed waterproofing membrane bonded on shotcrete can bridge cracks and fissures when deformation occurs (Holter 2014).

ITAtech (2013) has published design guidance for sprayed waterproofing membranes to provide tunnel designers, contractors, and owners with a comprehensive set of information about incorporating sprayed

∗Corresponding author, Senior Research Fellow
E-mail: sooho@kict.re.kr

ISSN: 2005-307X (Print), 2092-6219 (Online)

waterproofing membranes into composite tunnel linings. The document also suggests minimum performance requirements for sprayed waterproofing membranes and corresponding testing methods.

Previous studies on sprayed waterproofing membranes mainly discussed their mechanical properties, waterproofing performance, and moisture permeation to the shotcrete lining (Holter 2016, Holter and Foord 2015, Holter and Geving 2016, Holter *et al.* 2014). Su and Bloodworth (2016) stated that the mechanical properties of the shotcrete–membrane interface remain unclear, as they have yet to be investigated. Johnson *et al.* (2016) also noted the lack of systematic study on the effects of normal pressure on the shear strength of interface.

Therefore, this study aims to evaluate the interfacial properties of composite shotcrete containing a sprayed and bonded waterproofing membrane. Two EVA (ethyl-vinyl-acetate)-based membrane prototypes with different mixing conditions and mechanical properties were made to assess the effects of membrane properties on the interfacial behavior of composite shotcrete. They were then subjected to a series of direct shear and uniaxial compression tests to obtain shear stiffness at the interface of composite specimens and normal stiffness of composite specimens. The stiffness is a key input parameter for numerical models used to analyze and design tunnels with composite shotcrete linings. The shear stiffness of the interface in composite specimen is important in determining the degree of composite action between the primary and secondary linings, while the normal stiffness influences the amount of load that can be transferred between the primary and secondary linings at locations where the interface is under normal stress (Su and Bloodworth 2016). This study also observed the failure mechanism of both specimens' interfaces Finally, these failure mechanisms at the interface were investigated by visual inspection as well as three-dimensional X-ray CT scanning.

2. Performance deterioration caused by corrosion

2.1 Production of membrane prototypes

Two prototype waterproof membrane compositions were produced through a series of preliminary both tests (Table 1). Prototype 1 has two components, a liquid-type EVA polymer and powder materials, which were mixed at a 3:1 weight ratio in the hopper of a membrane spraying machine. This prototype was intended to reduce dust generated during membrane spraying. Prototype 2 is a powder-only mixture containing a powder-type EVA polymer and other powder materials. Before being sprayed, the pre-mixed powders are mixed in the nozzle of a spraying machine with water at a 1:3 weight ratio. Prototype 2 is cheaper to make and quicker to prepare than Prototype 1. The main component of both prototypes is EVA polymer, although in different forms.

Before the interfacial properties of the sprayed waterproofing membrane prototypes were evaluated, their physico-mechanical properties were evaluated by the suggested testing methods and minimum performance

Table 1 Chemical compositions of two kinds of spayed waterproofing membrane prototype (unit: weight %)

Materials	Prototype 1 (two-component)	Prototype 2 (one-component)
Alumina cement	30	15
Calcium sulfo-aluminate	30	-
Calcium carbonate	19.5	14.1
Slag	15	-
Nano silica	4	-
Lithium carbonate	0.1	-
Citric acid	0.3	-
Anhydrous gypsum	-	5
Hydroxypropyl methylcellulose	0.5	-
Antifoaming agent	0.3	-
Aluminum hydroxide	-	10
Thickener	-	0.85
Promoter	-	0.05
Synthetic fiber	0.3	-
Powder-type EVA polymer	-	55

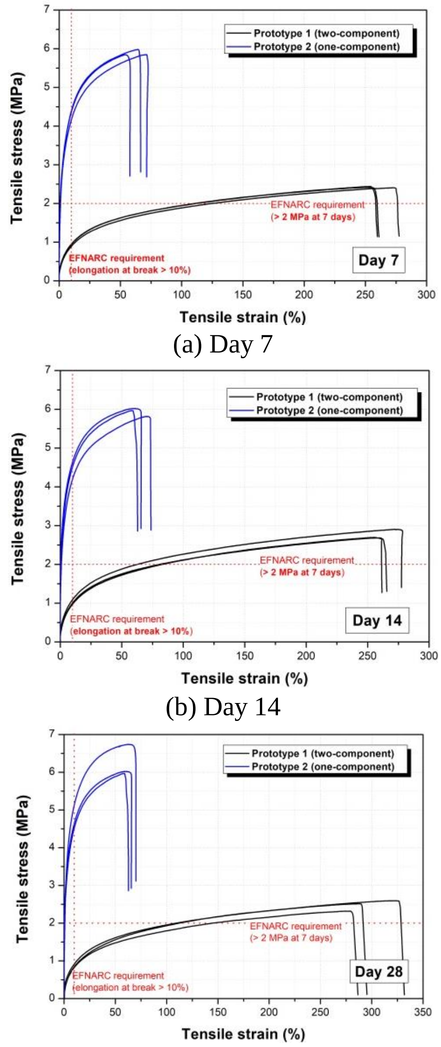

(a) Day 7

(b) Day 14

(c) Day 28

Fig. 1 Tensile stress-strain curves of membrane prototypes at different curing ages requirements (ITAtech 2013). While sprayed waterproofing membranes are not considered structural supports, only a waterproofing measure, they are potentially useful structural supports. Therefore, additional tests suggested by EFNARC (2008), which are widely used for the evaluation of thin spray-on liners (TSLs), were conducted for both membrane prototypes because the TSLs used as rock support members in mining have chemical compositions very close to those of a sprayed waterproofing membrane. All tests, including specimen production, were carried out under the same ambient temperature in the laboratory.

2.2 Tensile strength

ITAtech (2013) does not provide a requirement for the tensile strength of a sprayed waterproofing membrane. However, to evaluate fundamental mechanical properties of the prototype membranes, their tensile strengths were measured by the ASTM D638 (2010) standard testing method suggested by EFNARC (2008). This test employed prototype specimens with the thickness of 3 mm. The tensile stress-strain curves obtained for both prototypes at different curing ages are shown in Fig. 1. The tests confirm that both prototypes met the criteria proposed by EFNARC (2008): i.e., the tensile strength at 7 days must be more than 2 MPa and the elongation at break must be below 10% (see Figs 2-3).

Throughout the curing period, Prototype 1 was more ductile, with an elongation at break about six times that of Prototype 2. Prototype 2 had about twice the tensile strength of Prototype 1, and more brittle failure behavior (Figs. 2 and 3). Therefore, Prototype 1 might be much more favorable in field conditions requiring high ductility and flexibility, whereas Prototype 2 might be better in conditions demanding high tensile strength.

2.3 Bond strength

The bond strengths of the membranes were established in pull-off tests performed according to the standard procedure given by BS EN 1542 (1999). First, six concrete block specimens were made for the two membrane prototypes with different curing ages (7, 14, and 28 days) by following the mixing conditions given by BS EN 1766 (2000). They were then coated with a membrane 5 mm thick. Circular-shaped dollies 50 mm in diameter were strongly attached on the surface of the membrane using an epoxy resin adhesive. Finally, overcoring work around bonded dollies thus completed the preparation for pull-out test, which was conducted at a loading rate of 1–3 MPa/min.

The pull-off tests showed estimated average bond strengths of Prototypes 1 and 2 developed at 7 days to be 2.20 and 2.86 MPa, respectively. These values are significantly higher than the 0.5 and 1.0 MPa minimum bond strengths recommended by ITAtech (2013) and EFNARC (2008) at 28 days respectively. The prototypes' bond strengths were 2.67 and 3.89 MPa at 28 days, respectively, indicating a slight increase in bond strength with curing time. Overall, Fig. 4 shows that Prototype 2, with a higher tensile strength, had stronger bonding than Prototype 1.

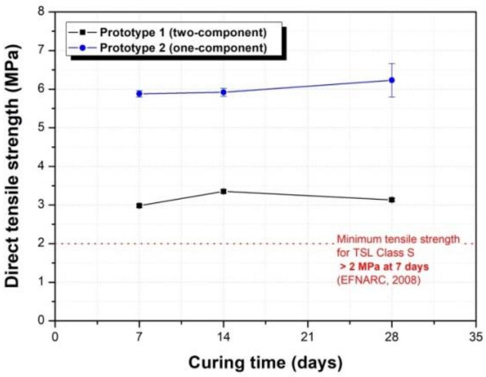

Fig. 2 Peak tensile strengths of membrane prototypes at different curing ages

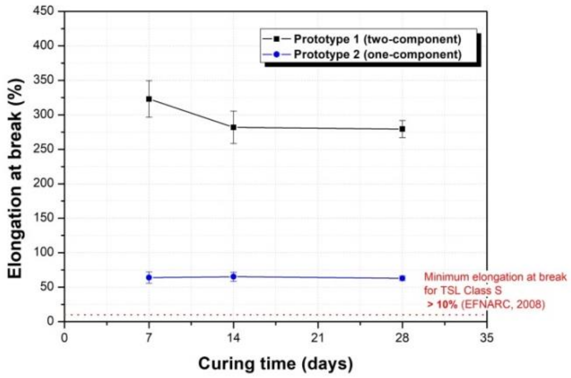

Fig. 3 Elongations at break of membrane prototypes at different curing ages

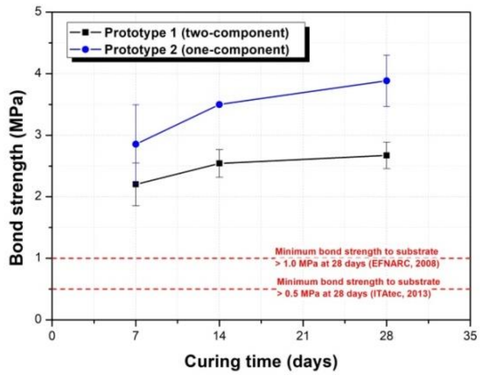

Fig. 4 Bond strengths of membrane prototypes at different curing ages

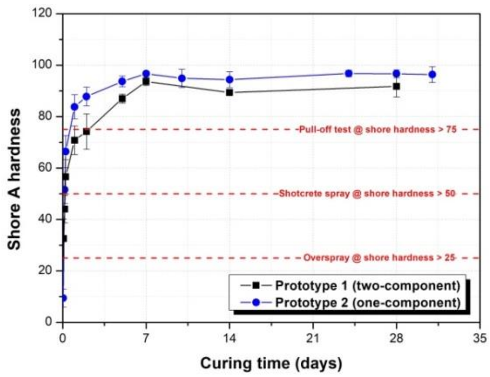

Fig. 5 Shore A hardness of membrane prototypes at different curing ages

2.4 Shore hardness

Even though ITAtech (2013) and EFNARC (2008) do not specify Shore hardness for the quality assurance of sprayed waterproofing membranes and TSL, respectively, Shore hardness was measured here at different curing ages of the membrane prototypes as an indirect evaluation of their workability. Shore A hardness was measured by the ASTM D2240 (2015) standard testing method. The sprayed membrane achieved a hardness level of 25 (Stubberfield 2016) only four hours after production. After six hours, the Shore A hardness reached 25 to 50, which is an acceptable level for the spraying of shotcrete onto the sprayed membrane (Stubberfield 2016). A Shore A hardness of 75 is considered suitable for bond strength measurement by pull-off testing (Stubberfield 2016), which was achieved after two days (Fig. 5). The Shore A hardness value converged to more than 90 after six days of curing.

Similar to previous results obtained from tensile strength and bond strength tests, Prototype 2 showed a higher Shore A hardness than Prototype 1.

2.5 Watertightness

The crucial property of the membranes' watertightness was evaluated by the EN 12390-8 method proposed by the ITAtech (2013) guidelines, which require there to be no penetration of water through a membrane for 28 days under a 3 bar water pressure. However, watertightness was assessed here at the higher level of 5 bars using the specimens and permeability testing system presented in Fig. 6. For the test, cylindrical porous concrete specimens were mixed by EN 14891 (2006): water-cement ratio ≥ 1.0, maximum grain size = 16 mm. Once the specimens were prepared, one side of each specimen was coated with the Prototype 1 with the thickness of 3 mm.

Fig. 7(a) shows membrane-coated specimens after 28 days of testing. The membrane was fastened with an O-ring and both plates of the testing system during testing. The O-ring was fully pressed down onto the membrane by the force from bolts for fixing the plates. No water penetration through the membrane was apparent on the porous concrete after removal of the membrane, as shown in Fig. 7(b).

Three-dimensional X-ray CT scanning was used for quantitative watertightness analysis of the membrane prototypes before and after the permeability tests. X-ray CT scanning is a non-destructive method that obtains a large number of consecutive sectional images of the internal micro-structure a specimen (Kim *et al*. 2012). The device used here was an X-EYE CT System (SEC Corporation, Korea) equipped with a micro-focus X-ray tube capable of attaining high spatial resolutions of up to 6.18 m^3. The voltage and current were set to 220 kV and 1,000 A, respectively. A CCD camera was used as a flat-panel detector to collect X-ray attenuation information after the radiation had passed through the specimen (Fig. 8). The detector measured 409.6 mm × 409.6 mm with a pixel pitch of 200 m and a limited resolution of 2.5 lp/mm (line pairs per millimeter). The maximum wobbling allowance of the manipulator, which determines the scanning location of the rotating specimen, was 5 mm. This value lies within the

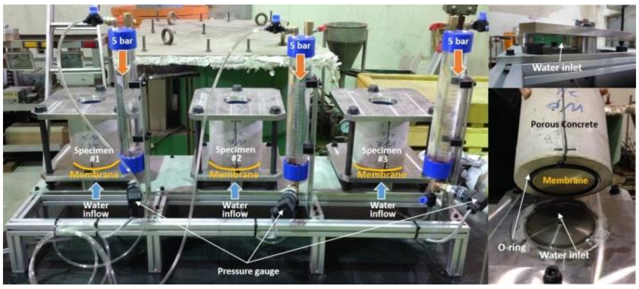

Fig. 6 Permeability testing system for sprayed waterproofing membranes

(a) Membrane coated specimens after 28 days

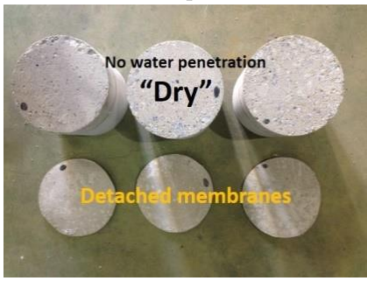

(b) Detached membranes and concrete specimens

Fig. 7 Investigation of water penetration through waterproofing membranes to porous concrete specimens after 28 days under 5 bars (Prototype 1)

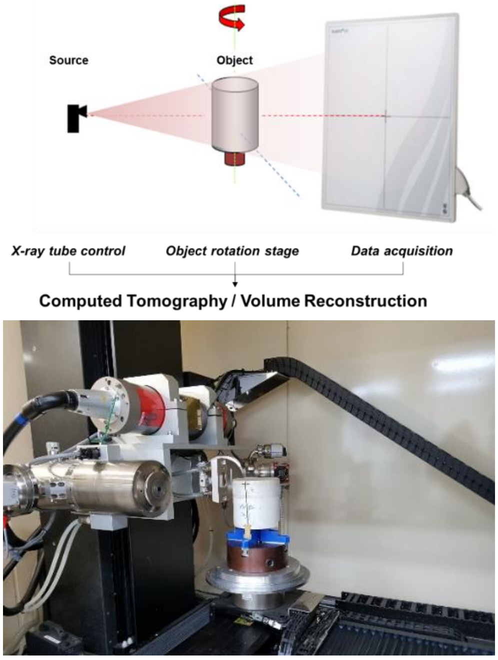

Fig. 8 Diagram and photograph of the X-ray CT scanning set-up

(a) 3D CT image

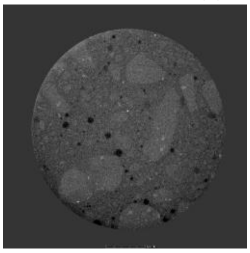

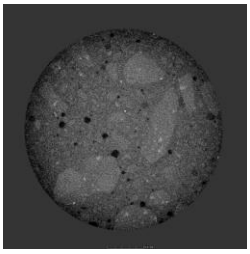

(b) Before test (c) After test

Fig. 9 Example of CT images of a concrete specimen before and after permeability testing for 28 days (Prototype 1)

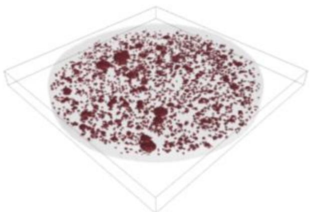

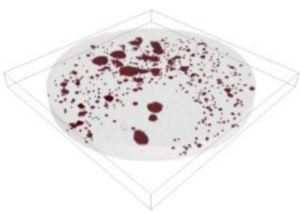

(a) Before test (b) After test

Fig. 10 Example of pore distribution within a waterproofing membrane before and after permeability testing for 28 days (Prototype 1)

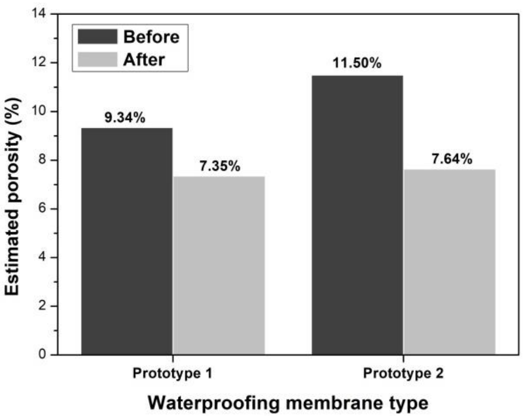

Fig. 11 Porosity of membrane prototypes estimated by three-dimensional X-ray CT scanning

range of correction ability during the reconstruction process (Chang *et al*. 2017, Kim *et al*. 2012). Each image had a pixel size of 0.2643 mm × 0.2653 mm with 1024 × 1024 pixels.

Fig. 9 displays three-dimensional CT images of concrete specimens coated with Prototype 1 membrane. Water penetration into the concrete is generally evidenced by the color of the pore image scanned by CT changing from black to almost gray owing to the different degrees of X-ray penetration into water and air. Therefore, Fig. 9(b) and 9(c) show no evidence of water penetration into the concrete specimen, except for the pores displayed as black circles. X-ray CT scanning of the membrane after the permeability test shows that a few pores in its inner part were saturated with water (Fig. 10). However, we surmised from scans obtained before the penetration test that these pores had been formed during the curing process of the membrane. Above all, it was difficult to detect inter-connected pores from the CT images. As summarized in Fig. 11, the average initial porosities of Prototype 1 and Prototype 2, estimated from three-dimensional X-ray CT scanning, were 9.34% and 11.50%, respectively. Therefore, although water was not capable of penetrating into the concrete specimen coated with the membrane, it was estimated that between about 21.3% and 33.6% of the entire pores in the membrane became saturated with water during the 28 days at 5 bar water pressure. Holter and Geving (2016) reported that EVA-based membranes exhibit significant water absorption although they are impermeable to liquid water flow. Holter (2016) also found that the in-situ moisture content of a membrane material varies within the range of 30%-40% of the maximum water absorption potential.

3. Preparation of composite specimens comprising sprayed concrete and membrane

For the evaluation of the interfacial properties between shotcrete and a sprayed waterproofing membrane, a direct shear test and uniaxial compression test were planned based on the concept as illustrated in Fig. 12. Before the tests, specimens were produced by spraying both the membrane and shotcrete. Mixing conditions of shotcrete with the design strength of 40 MPa was listed in Table 2.

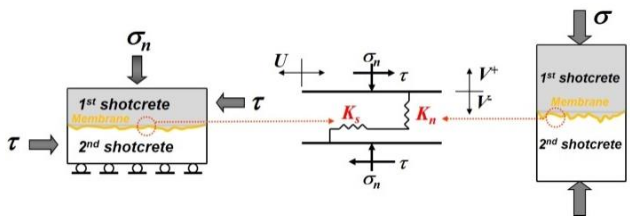

Fig. 12 Concept of evaluating the interfacial properties of shotcrete-membrane composite

Table 2 Mixing conditions for shotcrete for combined specimens with sprayed waterproofing membrane

W (Water) /B (Binder) (%)		38
S/a (Sand /aggregate) (Volume %)		65
Unit weight (kg/m^3)	W (Water)	182.5
	C (Cement)	456.0
	A (Silica fume)	24.0
	S (Fine aggregate)	1,127
	G (Coarse aggregate)	603
	Super-plasticizer	7.2
	Steel fiber	40
Alkali-free accelerator (%)		C x 8%

(a) First shotcrete spraying (b) Shotcrete curing

(c) Membrane spraying (d) Sprayed thickness check

(e) Second mold installation (f) Second shotcrete spraying

Fig. 13 Preparation of composite shotcrete specimens with sprayed waterproofing membrane

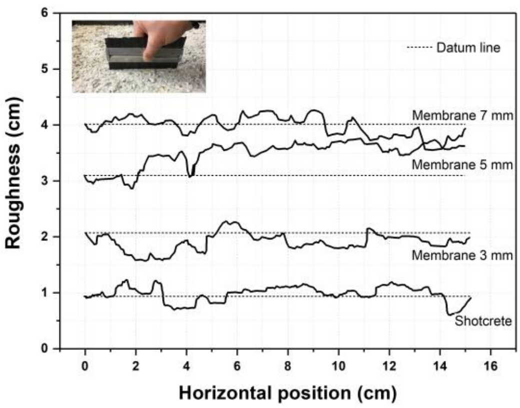

Fig. 14 Example roughness measured on surfaces of first shotcrete layer

Table 3 Measured membrane thickness after spraying

Target thickness	Measured thickness after spraying	
	Prototype 1	Prototype 2
3 mm	3.70±0.33 mm	3.67±0.59 mm
5 mm	5.86±1.49 mm	5.74±1.21 mm
7 mm	7.25±1.56 mm	7.16±1.38 mm

Fig. 13 describes the overall process of producing the shotcrete-membrane composite specimens. The first shotcrete layer (mixed as in Table 2) was sprayed to a thickness of about 7.5 cm into a custom-made steel panel mold (0.55 m × 0.55 m × 0.075 m (width × length × height)) placed at the tunnel construction site, as displayed in Fig. 13(a). The mold containing the shotcrete was moved to the laboratory and cured under an ambient temperature in the laboratory for 28 days as shown in Fig. 13(b). A profile gage measured its roughness as approximately ±1 mm (Fig. 14), which is appropriate for waterproofing membrane spraying (Stubberfield 2016).

Fig. 13(c) shows the spraying of both prototype membranes onto the surface of the first shotcrete layer. Prototype 1, the membrane made from liquid-type EVA polymer and various powders mixed at a 3:1 weight ratio in the hopper, was sprayed by a ICT 206 spraying machine. Prototype 2, made using only powdered components, was mixed in the hopper of a Meyco Piccola spraying machine and sprayed with water added in the nozzle at a weight ratio of 1:3. Membranes were sprayed at target thicknesses of 3, 5, and 7 mm to assess the influence of thickness on interfacial behavior. The actual thickness of each membrane prototype under wet conditions was measured directly after spraying (Fig. 13(d)), and found to deviate only slightly from the target values owing to the roughness of the underlying shotcrete (Table 3). After spraying, the membranes were cured for two days to reach a Shore A hardness above 50, which considered acceptable for further shotcrete spraying.

After curing, a second steel panel mold was applied onto the first (Fig. 13(e)), and similarly the secondary shotcrete layer was sprayed onto the surface of the membrane to a thickness of 7.5 cm (Fig. 13(f)). Double-layered specimens without any membrane, comprising only the first and second shotcrete layers, were produced for comparison to help understand the interfacial properties generated from the concrete and membrane.

Finally, after removal of the molds, we made five specimens (0.1 m × 0.1 m × 0.15 m (width × length × height)) of each of the three thicknesses for direct shear testing. Each new specimen was cut from the original, avoiding its corners. Specimens for uniaxial compression testing were cores (at least three) of 100 mm diameter per thickness obtained from the remainder of the original specimen left after cutting.

4. Evaluation of interfacial properties between shotcrete and sprayed waterproofing membrane

4.1 Direct shear tests

Direct shear testing was used to evaluate the interfacial shear behavior between the shotcrete and the sprayed waterproofing membrane. For Prototype 2 (i.e., specimens including double-layered shotcrete), 20 specimens were prepared for direct shear testing under five different constant normal-stress conditions (0.3, 0.6, 0.9, 1.2 and 1.5 MPa). For Prototype 1, nine composite specimens could be prepared for testing under three different normal-stress conditions (0.5, 1.0 and 1.5 MPa). The shear displacement rate associated with horizontal movement of the shear box was set to 1 mm/min for the entire test.

The primary results of the entire test are listed in Table 4. Fig. 15 presents typical direct shear stress-displacement curves for the interfaces in composite specimen with Prototype 2 membrane and in double-layered shotcrete.

The peak shear strengths of the interfaces in the composite specimen were estimated to be lower than those of the double-layered shotcrete under constant normal stress. Considering the peak shear strength of interface in each specimen, the residual shear strength generated at the

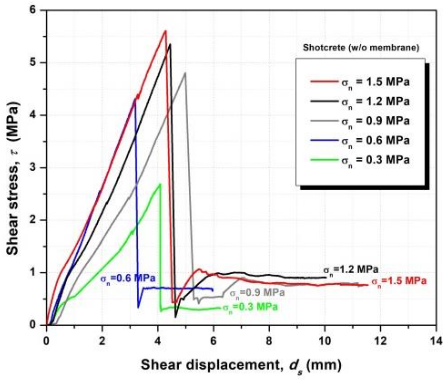

(a) Double-layered shotcrete

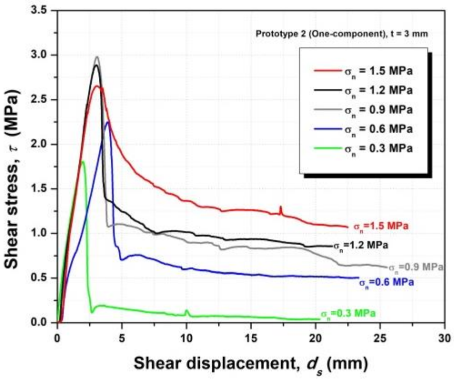

(b) Composite specimens (Prototype 2, t = 3 mm)

Fig. 15 Typical shear stress-displacement curves of the interfaces in shotcrete and composite specimens

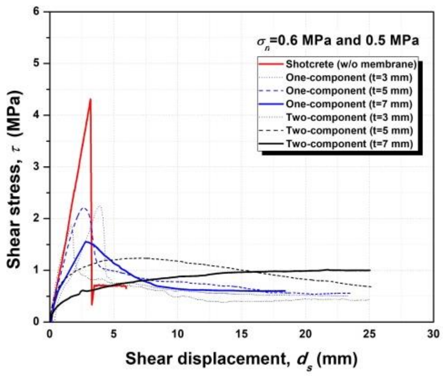

(a) σ_n = 0.5 and 0.6 MPa

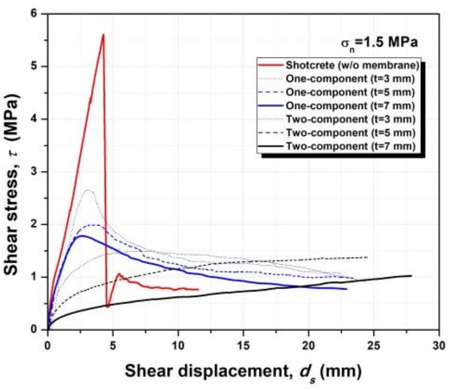

(b) σ_n = 1.5 MPa

Fig. 16 Shear stress-displacement curves of interfaces in shotcrete and composite specimens at different constant normal stress conditions

Table 4 Summary of direct shear tests on composite shotcrete specimens with sprayed membrane

Material	Normal stress, σ_n (MPa)	Peak shear strength, τ_{peak} (MPa)	Residual shear strength, τ_{res} (MPa)	Shear stiffness, K_s (GPa/m)	Displacement at failure, d_{fail} (mm)	Cohesion (MPa)	Peak friction angle (°)	Residual friction angle (°)
Double-layered shotcrete (No membrane)	0.3	2.69	0.31	0.54	4.09	2.49	66.50	34.95
	0.6	4.31	0.70	1.52	3.19			
	0.9	4.80	0.79	0.87	4.99			
	1.2	5.36	0.90	1.22	4.44			
	1.5	5.61	0.77	1.43	4.28			
Prototype 1 (t = 3 mm)	0.5	1.88	0.43	1.14	1.69	1.51	33.90	32.21
	1.0	2.11	0.71	1.16	1.97			
	1.5	2.84	0.84	1.74	1.62			
Prototype 1 (t = 5 mm)	0.5	0.89	Not clear	0.53	11.23	0.72	25.64	Not computable
	1.0	1.35		0.76	9.72			
	1.5	1.37		0.83	21.16			
Prototype 1 (t = 7 mm)	0.5	Not clear (continuously increasing)		0.32	Not computable	Not computable		
	1.0			0.39				
	1.5			0.51				
Prototype 2 (t = 3 mm)	0.3	1.81	0.04	0.95	1.99	1.82	37.72	45.49
	0.6	2.25	0.51	0.63	3.91			
	0.9	2.98	1.05	0.64	3.10			
	1.2	2.89	0.86	0.95	3.04			
	1.5	2.65	1.09	0.92	3.06			
Prototype 2 (t = 5 mm)	0.3	2.05	0.05	0.84	2.34	2.04	0	44.31
	0.6	2.21	0.55	0.91	2.64			
	0.9	2.06	0.67	0.78	2.69			
	1.2	1.89	1.15	0.60	4.33			
	1.5	1.99	1.00	0.89	3.72			
Prototype 2 (t = 7 mm)	0.3	1.61	0.33	0.77	2.31	1.57	8.16	34.13
	0.6	1.55	0.60	0.45	2.78			
	0.9	1.93	0.60	0.94	2.18			
	1.2	1.64	0.70	0.67	2.65			
	1.5	1.78	0.74	0.79	2.60			

interface of the composite was estimated to be much higher than that at the interface of the double-layered shotcrete after the failure. Moreover, the residual strength of the interfaces in the composite specimens tended to increase as the normal stress increased.

To compare the shear behavior of the composite specimen with that of the double-layered shotcrete, shear stress-displacement curves for both specimens under the same (1.5 MPa) and similar normal stress conditions (0.6 and 0.5 MPa) were derived. The results (Fig. 16) confirm that the peak shear strength tended to decrease as the membrane became thicker and the normal stress decreased. This was because of the membrane's high ductility compared with that of the shotcrete. In particular, the peak shear strength of the interface in the composite specimen with Prototype 1 membrane, which was more ductile than Prototype 2 membrane, showed marked reduction. For the

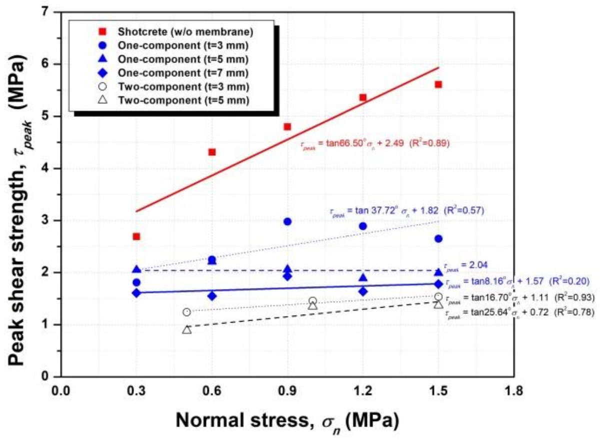

Fig. 17 Peak shear strengths of interfaces in composite and double-layered shotcrete specimens at different normal stress conditions

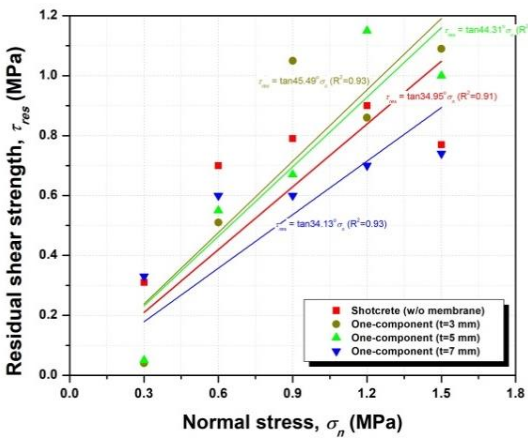

Fig. 18 Relationships between residual shear strength of the interface and normal stress

composite specimen with Prototype 1 membrane, it was more difficult to estimate the peak shear strength of the interface clearly because of its ductile and plastic behavior as the membrane became thicker, and the normal stress increased.

Fig. 17 shows the results of direct shear tests with the Mohr-Coulomb failure criterion. The normal stress and peak shear strength of the interface in double-layered shotcrete were linearly related, showing a cohesion of 2.49 MPa and peak friction angle of 66.5° (Table 4).

It was possible to estimate the cohesion and peak friction angle for the interface in the composite specimen with a 3-mm and 5-mm-thick Prototype 1 membrane, because of the clear linear relationship between normal stress and peak shear strength. Other samples (7-mm-thick Prototype 1 membrane), however, did not show an increasing trend between normal stress and the peak shear strength of the interface. Instead, it was nearly impossible to assess the peak shear stress for the interface of the composite specimen with the 7-mm-thick Prototype 1 membrane as the shear stress remained gradually increasing even as the shear displacement reached 25 mm.

The peak shear strength of the interface in the composite specimens with 7-mm-thick Prototype 2 membrane

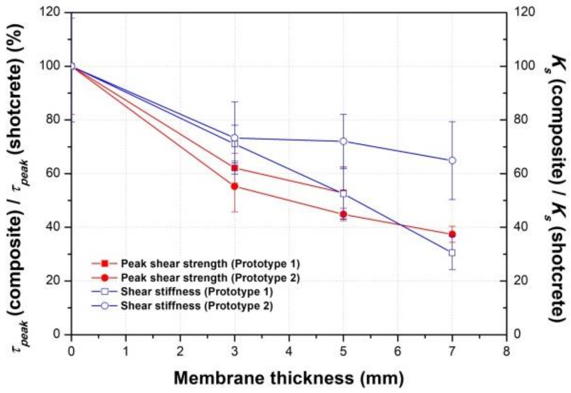

Fig. 19 Normalized peak shear strength and shear stiffness of interfaces depending on different membrane thicknesses

remained nearly constant at 1-2 MPa regardless of the normal stress. Hence, the peak and residual shear strength of this sample's interfaces were not measured. The interface of the composite specimen with the 5-mm-thick Prototype 2 membrane had peak shear strengths of 2 MPa under all normal stress conditions. It seems that the cohesion and peak friction angle of the interface in composite specimen decreased because of the growing influence of the membrane's ductility and flexibility as the membrane became thicker. Su and Bloodworth (2016) estimated the peak shear strengths of EVA-based membranes as 2-3.5 MPa under 0.5 MPa normal stress condition. Under same conditions, the peak shear strength and shear stiffness of the interface were estimated to be lower in the composite specimens than in the double-layered shotcrete. However, Vogel *et al*. (2017) noted that shear stress is not generated and transferred through the interface between conventional waterproofing sheets and the concrete. Although peak shear strengths of the interface in composite specimens were estimated to be 1-3 MPa lower than those of double-layered shotcrete specimens, it seems that the shear stress can be generated and transferred through the membrane layer of the composites. This conclusion is supported by previous studies (Johnson *et al.* 2016, Nakashima *et al.* 2015) that the thickness of composite shotcrete linings could be reduced and optimized by using a coated membrane, as significant load sharing and shear stress transfer are generated between the shotcrete and the sprayed waterproofing membrane.

As shown in Fig. 16, it was difficult to evaluate the peak and residual shear strength of the interface in the composite specimens with Prototype 1 membrane. However, the residual strength of the interface in the composite specimens with Prototype 2 membrane and the interface in double-layered shotcrete increased linearly as the normal stress increased (Fig. 18). By assuming that the interface failed at the peak stress, linear regression was conducted only for the residual friction angle. The test estimated residual friction angles of 34°-45° for the interfaces in both composite specimens with Prototype 2 membrane and the double-layered shotcrete. Despite the large deviation in the results, they show that the residual friction angle of the interface increased as the Prototype 2 membrane decreased

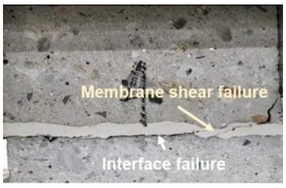

(a) at d_{fail} (t = 3 mm)

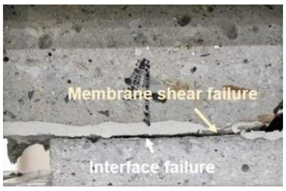

(b) at 600% of d_{fail} (t = 3 mm)

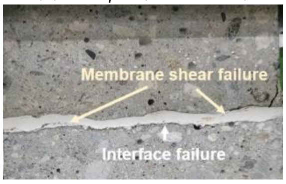

(c) at d_{fail} (t = 5 mm)

(d) at 600% of d_{fail} (t = 5 mm)

(e) at d_{fail} (t = 7 mm)

(f) at 600% of d_{fail} (t = 7 mm)

Fig. 20 Examples of failed specimens after direct shear tests (Prototype 2, σ_n = 0.9 MPa)

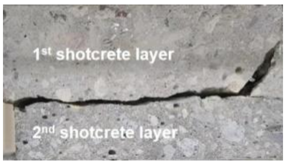

(a) at d_{fail}

(b) at 200% of d_{fail}

Fig. 21 Example of a failed shotcrete-only specimen after direct shear test (σ_n = 0.9 MPa)

in thickness. Except for the composite sample with the 7-mm-thick Prototype 2 membrane, the estimated residual friction angle of the interface was estimated to be higher in the composites than in the double-layered shotcrete.

Based on Table 4, Fig. 19 presents the relationship between normalized peak shear strength (or shear stiffness) and membrane thickness. Because no clear relationship between the normal stress and peak shear strength or shear stiffness was found, the average and deviation of all test results were presented without considering normal stresses. The peak shear strength and shear stiffness both decreased as the membrane became thicker; for the composites they were estimated to be 40%-60% and 30%-75%, respectively, of those of the shotcrete-only specimen. For highly ductile Prototype 1, the shear stiffness reduced more strongly than for Prototype 2 as the target thickness increased. As listed in Table 4, the shear stiffnesses of the interfaces in composite specimens were estimated to be 0.32-1.74 GPa/m under given normal stress conditions. Su and Bloodworth (2016) estimated shear stiffnesses to be 0.6 GPa/m under 0.25-0.75 MPa normal stress. Johnson *et al*. (2016) and Holter (2016) gave shear stiffness estimates of 0.39-0.5 GPa/m and 0.29-0.35 GPa/m, respectively, from studies under 0.25-0.75 MPa normal stress. Despite the different normal stress conditions between this study and the previous studies, the range of shear stiffness estimated here is generally close to those from earlier works.

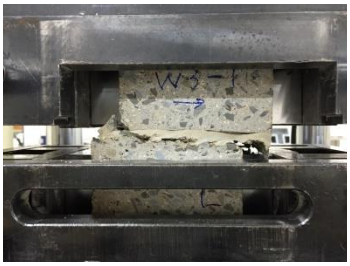

(a) Prototype 1 (t = 3 mm)

(b) Prototype 1 (t = 5 mm)

(c) Prototype 1 (t = 7 mm)

Fig. 22 Examples of failed specimens after direct shear tests (Prototype 1, σ_n = 0.5 MPa)

The failure mechanism of the specimens' interfaces was explored by examining their failure modes with respect to the shear displacement after peak shear stress (Figs. 20-22). The composite specimen with Prototype 2 membrane did not show cracks before the development of the peak shear stress. However, cracks were clearly observed after the peak shear stress. Visual inspection revealed two kinds of failure: shear failure at the interface and shear failure in the membrane. The former indicated the detachment of the membrane from the shotcrete layer (clearly shown in Fig. 20(f)), whereas the latter means that the membrane itself failed (Fig. 20(a)). Shear failure at the interface became dominant as the membrane layer increased in thickness, but it was difficult to determine which failure was dominant in samples with thin membranes under the same normal stress conditions (Fig. 20(a) and 20(c)). Moreover, the failure mechanism was not observed to depend on the normal stress conditions for a given thickness of membrane. Prototype 1 membrane had greater flexibility and was more elongate than Prototype 2 membrane (Fig. 3). Therefore, shear failure at the interface was observed more often in the composite specimens with Prototype 1 membrane than with Prototype 2 membrane under the same conditions (Fig. 22). As for the double-layered shotcrete, shear failure was generated on the interface between the two layers parallel to the shear direction.

To examine the failure surface in three dimensions, X-ray CT scanning was performed on the specimens used in the direct shear tests (i.e., those in Figs. 20 and 21). In Fig. 23, the red surface indicates the membrane and the dark cyan surface means the membrane failed and was torn off. Corroborating the visual observation, shear failure at the interface appears over a larger surface area than the shear failure in the membrane. This agrees with the observations of Su and Bloodworth (2016), who reported that although composite shotcrete specimens with a sprayed waterproofing membrane failed under a mixed mode of the shear failure at the interface and shear failure in membrane, the former dominated a by-product of the interface failure with shearing within the membrane.

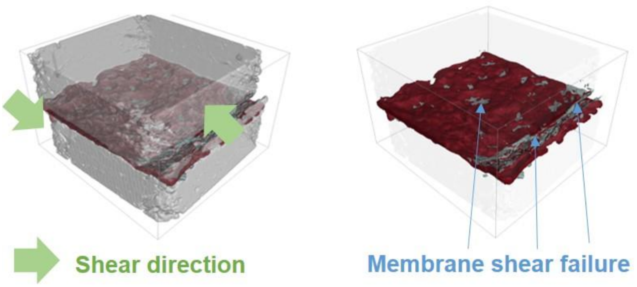

(a) Prototype 2 (t = 3 mm)

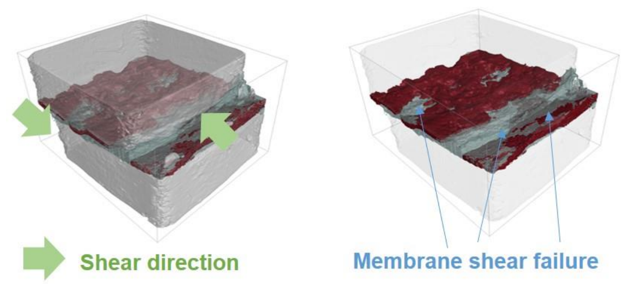

(b) Prototype 2 (t = 5 mm)

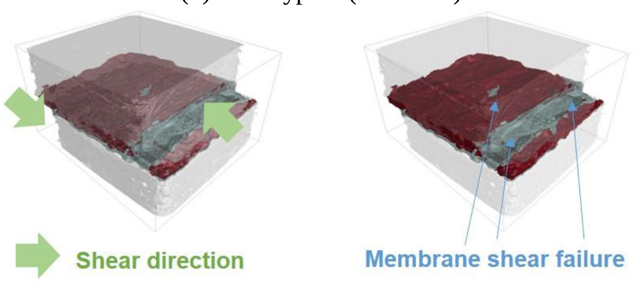

(c) Prototype 2 (t = 7 mm)

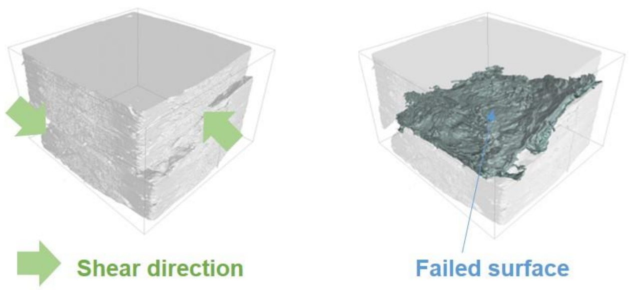

(d) Double-layered shotcrete

Fig. 23 Three-dimensional X-ray scan images of failed direct shear specimens (σ_n = 0.9 MPa)

Table 5 Summary of uniaxial compression tests on composite shotcrete specimens with sprayed membranes

Material	Uniaxial compressive strength, σ_c (MPa)	Normal stiffness, K_n (GPa/m)	Displacement at peak, d_{peak} (mm)
Double-layered shotcrete (No membrane)	55.06	110.63	0.68
	57.52	113.98	0.61
	58.36	107.83	0.70
	Avg. 56.98±1.81	Avg. 110.81±3.08	Avg. 0.66±0.05
Prototype 1 (t = 3 mm)	28.95	20.47	3.26
	30.69	21.81	3.74
	Avg. 29.82±0.87	Avg. 21.14±0.95	Avg. 3.50±0.24
Prototype 1 (t = 5 mm)	19.31	15.69	4.13
	28.75	11.58	3.96
	29.50	19.44	3.28
	Avg. 24.03±4.72	Avg. 15.57±3.93	Avg. 3.79±0.37
Prototype 1 (t = 7 mm)	21.33	5.16	5.44
	19.11	5.07	6.56
	Avg. 20.22±1.11	Avg. 5.12±0.06	Avg. 6.00±0.56
Prototype 2 (t = 3 mm)	29.17	17.41	2.04
	37.71	27.02	1.79
	38.57	29.36	1.99
	Avg. 35.15±5.20	Avg. 24.60±6.33	Avg. 1.94±0.13
Prototype 2 (t = 5 mm)	35.77	21.16	2.18
	31.84	13.85	2.75
	30.64	16.29	2.91
	Avg. 32.75±2.68	Avg. 17.10±3.72	Avg. 2.61±0.38
Prototype 2 (t = 7 mm)	22.65	10.15	2.79
	28.43	9.53	3.47
	20.23	7.44	3.54
	Avg. 23.77±4.21	Avg. 9.04±1.42	Avg. 3.27±0.41

4.2 Uniaxial compression tests

Uniaxial compression tests were used to evaluate the compressive strengths of the composite specimens (Table 5). For each compression test, the sprayed membrane was located perpendicular to the loading direction and in the middle of each cylindrical composite specimen.

Fig. 24 presents typical axial stress-displacement curves of composite specimens with Prototype 2 membrane derived from the tests. Similar to as observed in direct shear tests, the estimated peak normal strength and normal stiffness of the composites specimens were lower than those of the double-layered shotcrete. As the sprayed membrane became thicker, the normal stiffnesses of the composite specimens became much lower than those of double-layered shotcrete specimens, and it decreased more dramatically than the shear stiffnesses in the direct shear tests.

Fig. 25 compares the uniaxial compressive strength and normal stiffness of specimens with and without membranes of various thickness. As the membrane layer increased in thickness, the uniaxial compressive strengths of the

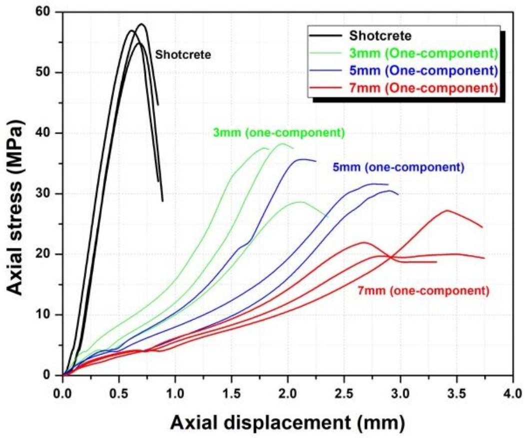

Fig. 24 Axial stress-displacement curves from compression tests (Prototype 2)

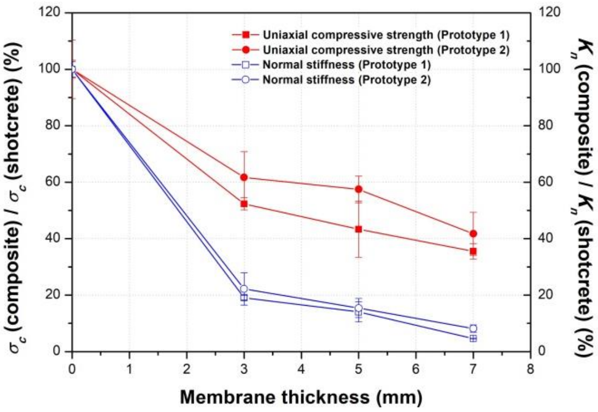

Fig. 25 Normalized compressive strength and normal stiffness for different membrane thicknesses

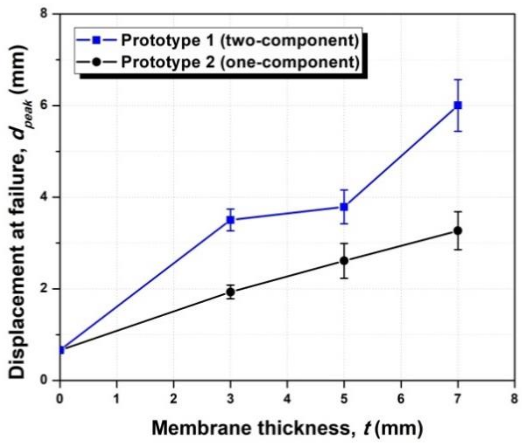

Fig. 26 Displacement at failure dependent on membrane thickness from uniaxial compression tests

composite specimens decreased to 35%-62% of those of the double-layered shotcrete specimens. However, the normal stiffness of the composite specimen was estimated to be 5%-22% of that of the double-layered shotcrete specimen, indicating that the composites' normal stiffness showed a greater decrease (relative to that of the double-layered shotcrete) than the shear stiffness.

Fig. 24 presents typical axial stress-displacement curves

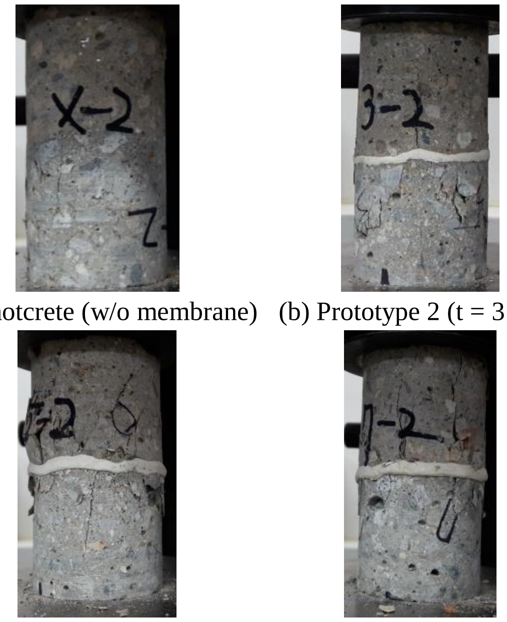

(a) Shotcrete (w/o membrane) (b) Prototype 2 (t = 3 mm)

(c) Prototype 2 (t = 5 mm) (d) Prototype 2 (t = 7 mm)

Fig. 27 Examples of failed specimens after uniaxial compression tests

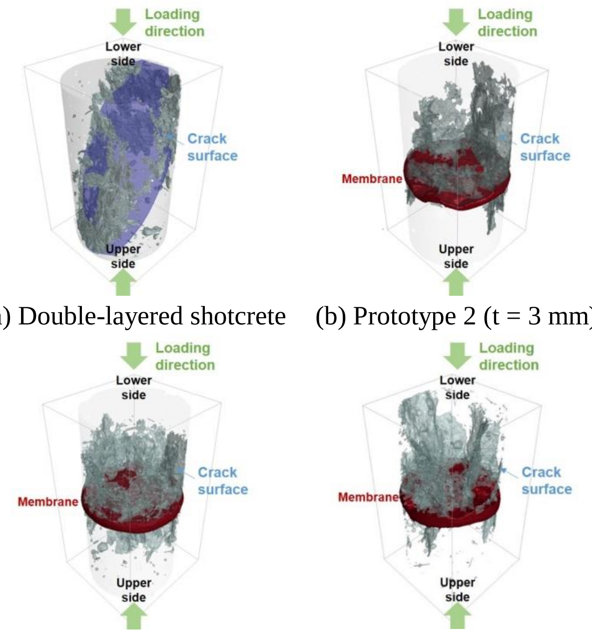

(a) Double-layered shotcrete (b) Prototype 2 (t = 3 mm)

(c) Prototype 2 (t = 5 mm) (d) Prototype (t = 7 mm)

Fig. 28 X-ray CT images of cracks generated in specimens under uniaxial compression

of composite specimens with Prototype 2 membrane derived from the tests. Similar to as observed in direct shear tests, the estimated peak normal strength and normal stiffness of the composites specimens were lower than those of the double-layered shotcrete. As the sprayed membrane became thicker, the normal stiffnesses of the composite specimens became much lower than those of double-layered shotcrete specimens, and it decreased more dramatically than the shear stiffnesses in the direct shear tests.

Fig. 25 compares the uniaxial compressive strength and normal stiffness of specimens with and without membranes of various thickness. As the membrane layer increased in thickness, the uniaxial compressive strengths of the composite specimens decreased to 35%-62% of those of the double-layered shotcrete specimens. However, the normal stiffness of the composite specimen was estimated to be 5%-22% of that of the double-layered shotcrete specimen, indicating that the composites' normal stiffness showed a greater decrease (relative to that of the double-layered shotcrete) than the shear stiffness.

In particular, the compressive strength and normal stiffness of the composite specimen decreased more as the membrane became thicker and more ductile. In the direct shear test, the strong bonding force was acted on the interface between the membrane and shotcrete nearly parallel to the shear failure plane. On the other hand, in the uniaxial compression test, the compressive loading was applied normal to the surface. Hence, the uniaxial compressive strength and normal stiffness of the composite specimens decreased, and the normal displacement of the composite specimens increased before failure occurred, because the membrane was much more flexible and softer than the shotcrete. In addition, as Prototype 1 was more flexible and ductile than Prototype 2, the composite specimens with Prototype 1 failed with a larger displacement than the composite specimens with Prototype 2 (Fig. 26).

As listed in Table 5, the normal stiffnesses of the composites were estimated to be 5-24 GPa/m depending on the membrane thickness. Verani and Aldrian (2010) used a finite difference code, FLAC, to model the primary and secondary linings of a circular tunnel with an interface with a normal stiffness of 17 GPa/m. Su and Bloodworth (2016) also reported that the compressive normal stiffness of composite specimens ranged from 1-16 GPa/m from a series of compression tests. Vogel *et al*. (2017) assumed the normal stiffness of a two-dimensional interface numerical model to be 4 GPa/m. Therefore, the range of normal stiffness seen here seems to be similar to previously reported values.

Fig. 27(b), 27(c) and 27(d) show that the composite specimens failed under the compressive force with the formation of the transverse tension cracks, mainly around the concrete surface perpendicular to the membrane layer. Moreover, the membrane was laterally squeezed out by the compressive force normal to its plane. Su and Bloodworth (2016) stated that during the compression of the composite specimen, the additional horizontal tension strains were induced at the interface by the squeezed membrane. Therefore, it seems that the peak strength of the composite specimen was developed lower than that of the double-layered shotcrete specimen (Fig. 24).

Finally, the three-dimensional X-ray CT scanning was carried out for failed specimens with Prototype 2 membrane. The scans show that many induced vertical cracks were concentrated on the surface of the composite specimen. Moreover, more cracks were found in the lower part of the specimen than in the upper part (Fig. 28).

5. Conclusions

This study undertook experiments to evaluate the interfacial properties of composite shotcrete specimens with sprayed waterproofing membranes by direct shear and uniaxial compression tests. Both types of sprayed waterproofing membrane prototype based on EVA polymers were found to be satisfactory for use as waterproofing and rock support, as they satisfied minimum performance requirements suggested by ITAtech (2013) and EFNARC (2008).

The test for the minimum performance requirements showed Prototype 1 (composed of a liquid-type EVA polymer and powder mixture) to be much more ductile and flexible behaviors than Prototype 2 (made from a powder-type EVA polymer).

The average initial porosities of Prototype 1 and Prototype 2 were estimated to be 9.34% and 11.50% respectively, by three-dimensional X-ray CT scanning. It was also observed that 21.3%-33.6% of the initial pores were partially filled or saturated with water, although both membrane prototypes remained waterproof under a water pressure of 5 bar for 28 days.

Direct shear test of composite specimens with both prototype membranes showed their peak shear strengths and shear stiffnesses of the interfaces in composite specimens to decrease as the membrane layer became thicker under a constant normal stress. In particular, the peak shear strengths at the interface of the composite specimens were estimated to be 1-3 MPa at normal stresses of 0.3-1.5 MPa. Hence, the shear stress was clearly transferred at the interface between the shotcrete and the membrane. The shear stiffness, a critical input parameter for numerical analysis, ranged from 0.32-1.74 GPa/m under the given normal stress levels from 0.3-1.5 MPa. In addition, shear failure at the interface was dominant in samples with thicker and more flexible and ductile membranes under constant normal stress. Parameters for the interface between the sprayed membrane and shotcrete derived from the test are summarized in Table 6.

Table 6 Suggested values of parameters for interfacial properties between developed membrane and shotcrete

Membrane type	Target thickness (mean±deviation)	Shear stiffness (GPa/m)
Prototype 1 (Two component)	3 mm (3.70 mm±0.33 mm)	1.34±0.28
	5 mm (5.86 mm±1.49 mm)	0.71±0.13
	7 mm (7.25 mm±1.56 mm)	0.41±0.08
Prototype 2 (One component)	3 mm (3.67 mm±0.59 mm)	0.82±0.15
	5 mm (5.74 mm±1.21 mm)	0.80±0.11
	7 mm (7.16 mm±1.38 mm)	2.50±0.22

All composite specimens failed under compression via the formation of transverse tension cracks, mainly around the shotcrete surface perpendicular to the membrane layer. As the membrane was much more flexible and ductile than shotcrete, it was easily compressed and squeezed out by compressive loading perpendicular to its surface. Above all, additional horizontal tension strains were induced at the interface by the squeezed membrane during compression. Therefore, the peak strength of the composite specimen was lower than that of the double-layered shotcrete specimen.

In summary, a sprayed waterproofing membrane that is as thin as possible might be preferable to obtain higher strength and stiffness at the interface, provided its watertightness is guaranteed, even though the composite specimens were shown to have strength and stiffness values that were sufficient for shear stress transfer at the interface of two shotcrete layers and the membrane. To verify how to optimize composite shotcrete linings of this type by reducing their thickness, further studies are necessary to quantitatively evaluate the shear stress transfer and load sharing between the membrane and shotcrete layer, depending on the thickness of the shotcrete layer. In addition, further investigation should explore the effects of the roughness of the interface between the shotcrete and membrane under various normal stress conditions.

Acknowledgements

This work was financially supported by the Korea Agency for Infrastructure Technology Advancement under the Ministry of Land, Infrastructure and Transport of the Korean government. (Project Number: 17SCIP-B108153-03).

References

ASTM (2010), *Standard Test Method for Tensile Properties of Plastics*, ASTM D638-10.

ASTM (2015), *Standard Test Method for Rubber Property Durometer Hardness*, ASTM D2240-15.

BS EN 1542:1999 (1999), *Products and Systems for the Protection and Repair of Concrete Structures, Test Methods, Measurement of Bound Strength by Pull-Iff*.

BS EN 1766: 2000 (2000), *Products and Systems for the Protection and Repair of Concrete Structures, Test Methods, Reference Concretes for Testing*.

Chang, S.H., Lee, C., Kang, T.H., Ha, T. and Choi, S.W. (2017), "Effect of hardfacing on wear reduction of pick cutters under mixed rock conditions", *Geomech. Eng.*, **13**(1), 141-159.

EFNARC (2008), *Specification and Guidelines on Thin Spray-on Liners for Mining and Tunnelling*, ENC 250TSL v7.2 25-07-08.

EN 12390-8 (2009), *Testing Hardened Concrete—Part 8: Depth of Penetration of Water under Pressure*.

EN 14891 (2006), *Liquid Applied Water Impermeable Products for Use beneath Ceramic Tiling Bonded with Adhesives-Requirements, Test Methods, Evaluation of Conformity, Classification and Designation*.

Holter, K.G. (2014), "Loads on sprayed waterproof tunnel linings in jointed hard rock: A study based on Norwegian cases", *Rock Mech. Rock Eng.*, **47**(3), 1003-1020.

Holter, K.G. (2016), "Performance of EVA-based membranes for SCL in hard rock", *Rock Mech. Rock Eng.*, **49**(4), 1329-1358.

Holter, K.G. and Foord, R. (2015), "Testing of properties and constructability considerations of EVA-based sprayed membranes for waterproofing of tunnels", *Proceedings of the ITA WTC 2015 Congress and 41st General Assembly*, Dubrovnik, Croatia.

Holter, K.G. and Gerving, S. (2016), "Moisture transport through sprayed concrete tunnel linings", *Rock Mech. Rock Eng.*, **49**(1), 243-272.

Holter, K.G., Nilsen, B., Langas, C. and Tandberg, M.K. (2014), "Testing of sprayed waterproofing membranes for single shell sprayed concrete tunnel linings in hard rock", *Proceedings of the World Tunnel Congress 2014 and 40th ITA-AITES General Assembly*, Iguassu Falls, Brazil, May.

ITAtech (2013), *Design Guidance for Spray Applied Waterproofing Membranes*, ITAtech Report No. 2, ISBN 978-2-9700858-1-2.

Johnson, R.P., Swallow, F.E. and Psomas, S. (2016), "Structural properties and durability of a sprayed waterproofing membrane for tunnels", *Tunn. Undergr. Sp. Technol.*, **60**, 41-48.

Kim, K.Y., Yun, T.S., Choo, J., Kang, D.H. and Shin, H.S. (2012), "Determination of air-void parameters of hardened cement-based materials using X-ray computed tomography", *Construct. Build. Mater.*, **37**, 93-101.

Nakashima, M., Hammer, A.L., Thewes, M., Elshafie, M. and Soga, K. (2015), "Mechanical behavior of a sprayed concrete lining isolated by a sprayed waterproofing membrane", *Tunn. Undergr. Sp. Technol.*, **47**, 143-152.

Stubberfield, K. (2016), *Masterseal 345® Application Course – Lecture Material*, Tunnelling & Underground Construction Academy (TUCA), London, U.K., April 13, 2016.

Su, J. and Bloodworth, A. (2016), "Interface parameters of composite sprayed concrete linings in soft ground with spray-applied waterproofing", *Tunn. Undergr. Sp. Technol.*, **59**, 170-182.

Thomas, A. (2009) *Sprayed Concrete Lined Tunnels*, Taylor & Francis, London, U.K.

Verani, C.A. and Aldrian, W. (2010), *Composite Linings: Ground Support and Waterproofing through the Use of a Fully Bonded Membrane*, in *Shotcrete: Element of a System*, Taylor & Francis, London, U.K., 269-282.

Vogel, F., Sovjak, R. and Peskova, S. (2017), "Static response of double shell concrete lining with a spray-applied waterproofing membrane", *Tunn. Undergr. Sp. Technol.*, **68**, 106-112.

GC